Continuum and multiscale models of particle transport

Scott MacLachlan
scott.maclachlan@tufts.edu

Christoph Börgers and Stephanie Friedhoff

Tufts University

October 3, 2012

Charged particle transport

Interest originated with radiation dose planning problem:

Given a known tumor within a patient, calculate a radiation beam configuration to irradiate the tumor while not harming nearby tissue.

Key assumption:

- Know tumor and healthy tissue locations and scattering properties

Constrained optimization problem

In general, the radiation dose planning problem takes the form of an optimization problem,

$$\min_{g:Lf=g} J(f),$$

where

- g describes the geometry and properties of the radiation beams
- f is the phase-space density of particles per unit volume
- $J(f)$ is a given cost function
- $Lf = g$ is the linear Boltzmann Transport Equation

In order to solve this optimization problem, need to be able to solve forward problem, $Lf = g$

Phase-space density

$f = f(\mathbf{x}, \mathbf{v}, E, t)$ is the *phase-space density* of particles

Consider

$$\int_{t_0}^{t_1} \int_{E_0}^{E_1} \int_{\Omega_\mathbf{v}} \int_{\Omega_\mathbf{x}} f(\mathbf{x}, \mathbf{v}, E, t) d\mathbf{x} d\mathbf{v} dE dt,$$

modeling the number of particles

- with energy, E, satisfying $E_0 < E < E_1$
- passing through volume of space $\Omega_\mathbf{x}$
- moving in directions, $\mathbf{v} \in \Omega_\mathbf{v}$
- during the time interval $t_0 < t < t_1$

Linear Boltzmann transport equation

With $f = f(\mathbf{x}, \mathbf{v}, E, t)$, $Lf = g$ takes the form

$$\frac{1}{c}\frac{\partial f}{\partial t} + \mathbf{v} \cdot \nabla f + \sigma_t(\mathbf{x}, E) f - \mathcal{K}_s f = 0$$

$$f(\mathbf{x}, \mathbf{v}, E, t_0) = f_0(\mathbf{x}, \mathbf{v}, E)$$

$$f(\mathbf{x}, \mathbf{v}, E, t) = g(\mathbf{x}, \mathbf{v}, E, t) \text{ for } \mathbf{x} \in \partial\Omega$$

where

- the phase-space density, f, is a function of particle location, $\mathbf{x}$, direction of travel, $\mathbf{v}$, energy, E, and time, t
- c is the particle speed
- σ_t is the probability of interaction per unit of distance traveled, $\sigma_t = \left(\overline{\lambda}\right)^{-1}$ for mean free path $\overline{\lambda} > 0$
- $\mathcal{K}_s$ is the scattering kernel

Other applications

Boltzmann equation models many other transport regimes

- Electron microscopy
- Neutron transport (reactor design)
- interstellar radiation

Fundamental differences in $\mathcal{K}_s$ describe different regimes

Particle-based simulation

Natural to simulate using discrete particles

Seed domain with N particles, with initial positions, velocities, and energies distributed to statistically match $f_0(\mathbf{x}, \mathbf{v}, E)$

- independently integrate each particle at each time-step
- select particles at random (based on mean free path of travel) to interact with background
- reintroduce interacting particles based on scattering kernel

Particle-based simulation allows very effective parallelization

Is that it?

Particle-based simulation is

- Easy
- Cheap per particle
- Natural parallelization over particles

Why do anything else?

Is that it?

Particle-based simulation is

- Easy
- Cheap per particle
- Natural parallelization over particles

Why do anything else?

Particle-based simulations offer low accuracy relative to number of particles

Room for continuum modeling

Low accuracy of particle-based simulations opens door for other approaches

Back-of-the-envelope calculation suggests accurate grid-based discretization of PDE can yield better efficiency at high accuracy if optimal linear solvers are available

Philosophy:

- Revisit continuum model
- Look for opportunities for accurate grid-based discretization and fast solvers

---

C. Börgers, Phys. Med. Biol. 1998, **43**:517-528

Room for continuum modeling

Low accuracy of particle-based simulations opens door for other approaches

Back-of-the-envelope calculation suggests accurate grid-based discretization of PDE can yield better efficiency at high accuracy if optimal linear solvers are available

Philosophy:

- Revisit continuum model
- Look for opportunities for accurate grid-based discretization and fast solvers
- Start simple

C. Börgers, Phys. Med. Biol. 1998, **43**:517-528

Introduce assumptions

$$\frac{1}{c}\frac{\partial f}{\partial t} + \mathbf{v}\cdot\nabla f + \sigma_t(\mathbf{x}, E)f - \mathcal{K}_s f = 0$$

$$f(\mathbf{x}, \mathbf{v}, E, t_0) = f_0(\mathbf{x}, \mathbf{v}, E)$$

$$f(\mathbf{x}, \mathbf{v}, E, t) = g(\mathbf{x}, \mathbf{v}, E, t) \text{ for } \mathbf{x} \in \partial\Omega$$

- time-independent case, $\frac{\partial f}{\partial t} = 0$
- E, c are constant (mono-energetic transport)
- $\mathcal{K}_s f = \left(\overline{\lambda}\right)^{-1} p * f$, for some convolution kernel, p
  - all interactions result in scattering

Flatland model

Additionally, consider transport in only 2 spatial dimensions:

$$\mathbf{v} = (\cos(\theta), \sin(\theta))^T \text{ for } -\pi < \theta \leq \pi$$

Picture:

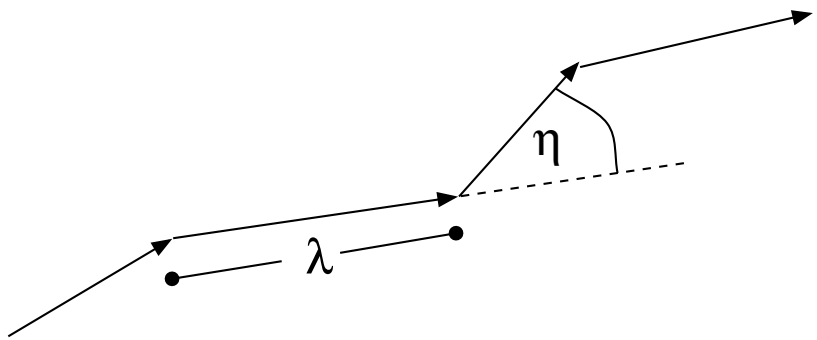

- Intercollision distances, λ, are independent, exponentially distributed with expectation $\overline{\lambda}$
- Scattering angles, η, are independent of each other and of λ

E.A. Abbott, *Flatland: a romance of many dimensions*, 1884

Model scattering kernel

Scattering for electron beams is highly forward peaked

- Let $p(\eta)$ be probability density for scattering with angle η
- $\mathcal{K}_s f = \left(\overline{\lambda}\right)^{-1} p * f = \left(\overline{\lambda}\right)^{-1} \int_{-\pi}^{\pi} p(\eta) f(\mathbf{x}, \theta - \eta) d\eta$

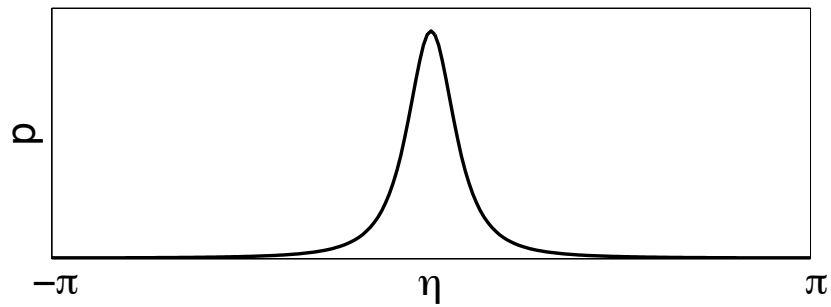

Compare to Neutron transport:

$$\mathcal{K}_s f = \sigma_s \int_{-\pi}^{\pi} f(\mathbf{x}, \theta - \eta) d\eta$$

for scattering cross-section σ_s.

Scattering kernels

Consider three example kernels

1. $\mathcal{K}_s f = \left(\overline{\lambda}\right)^{-1} p * f$ with $p(\eta) = \dfrac{C}{(2(1-\cos\eta)+\varepsilon^2)^{3/2}}$
   - Analogous to screened Rutherford scattering
2. $\mathcal{K}_s f = \left(\overline{\lambda}\right)^{-1} p * f$ with $p(\eta) = \dfrac{C}{(2(1-\cos\eta)+\varepsilon^2)}$
   - Analogous to Henyey-Greenstein scattering
3. $\mathcal{K}_s f - f/\overline{\lambda} = k f_{\theta\theta}$
   - Fokker-Planck scattering

The Fokker-Planck limit

$$\cos(\theta) f_x + \sin(\theta) f_y = \frac{p * f - f}{\overline{\lambda}} = Qf$$

C. Börgers, J. Comput. Phys. 1997, **133**:323-339

The Fokker-Planck limit

$$\cos(\theta) f_x + \sin(\theta) f_y = \frac{p * f - f}{\overline{\lambda}} = Qf$$

When $p(\eta)$ is small everywhere except near $\eta = 0$,

$$\begin{aligned} Qf &= \frac{1}{\overline{\lambda}} \left(\int_{-\pi}^{\pi} p(\eta) f(\theta - \eta) d\eta - f(\theta) \right) \\ &\approx \frac{1}{\overline{\lambda}} \left(\int_{-\pi}^{\pi} p(\eta) \left(f(\theta) - f_\theta(\theta)\eta + f_{\theta\theta}(\theta)\frac{\eta^2}{2} \right) d\eta - f(\theta) \right) \\ &= k f_{\theta\theta}(\theta) \end{aligned}$$

for $k = \frac{1}{2\overline{\lambda}} \int_{-\pi}^{\pi} \eta^2 p(\eta) d\eta$

In limit as $\overline{\lambda} \to 0$ and $\int_{-\pi}^{\pi} \eta^2 p(\eta) d\eta \to 0$, $Qf \rightharpoonup k f_{\theta\theta}$

C. Börgers, J. Comput. Phys. 1997, **133**:323-339

Mixed elliptic-hyperbolic operator

$$\cos(\theta) f_x + \sin(\theta) f_y = \frac{p * f - f}{\overline{\lambda}} = Qf$$

Operator has mixed character

- Left-hand side has hyperbolic character in x and y
- Right-hand side, Qf, is always negative definite
  - $Qf \rightharpoonup k f_{\theta\theta}$ in appropriate limit

Goal: develop a fast solver for accurate discretizations of this equation

Mixed elliptic-hyperbolic operator

$$\cos(\theta) f_x + \sin(\theta) f_y = \frac{p * f - f}{\overline{\lambda}} = Qf$$

Operator has mixed character

- Left-hand side has hyperbolic character in x and y
- Right-hand side, Qf, is always negative definite
  - $Qf \rightharpoonup k f_{\theta\theta}$ in appropriate limit

Goal: develop a fast solver for accurate discretizations of this equation

Large body of literature on accurate discretization for Boltzmann Transport

Start with the simplest possible one

Discretization in angle

Define Fourier coefficients,

$$\hat{p}_n = \int_{-\pi}^{\pi} e^{-in\eta} p(\eta)\, d\eta, \text{ and } \hat{f}_n = \frac{1}{2\pi} \int_{-\pi}^{\pi} e^{-in\tau} f(\tau)\, d\tau,$$

so that

$$Qf(\theta) = \sum_{n=-\infty}^{\infty} \frac{\hat{p}_n - 1}{\overline{\lambda}} \hat{f}_n \exp(in\theta).$$

Discretization in angle

Define Fourier coefficients,

$$\hat{p}_n = \int_{-\pi}^{\pi} e^{-in\eta} p(\eta)\, d\eta, \text{ and } \hat{f}_n = \frac{1}{2\pi} \int_{-\pi}^{\pi} e^{-in\tau} f(\tau)\, d\tau,$$

so that

$$Qf(\theta) = \sum_{n=-\infty}^{\infty} \frac{\hat{p}_n - 1}{\overline{\lambda}} \hat{f}_n \exp(in\theta).$$

Define $\Delta\theta = \frac{2\pi}{n_\theta}$, and $\Gamma_{n_\theta} = \{\theta_l = l\Delta\theta \mid -\frac{n_\theta}{2} + 1 \leq l \leq \frac{n_\theta}{2}\}$.
Discretize $f(\mathbf{x}, \theta)$ in angle by writing $\mathbf{f} = f(\mathbf{x}, \theta_l)$ for $\theta_l \in \Gamma_{n_\theta}$, giving

$$\left(Q^{\Delta\theta}\mathbf{f}\right)_l = \frac{1}{n_\theta} \sum_{n=-n_\theta/2+1}^{n_\theta/2} \sum_{m=-n_\theta/2+1}^{n_\theta/2} \frac{\hat{p}_n - 1}{\overline{\lambda}} \cos(n(\theta_l - \theta_m)) f(\theta_m)\,.$$

Discretization in space

For each θ_l, equation in x and y is simply advection:

$$\cos(\theta_l) f_x + \sin(\theta_l) f_y = (Q^{\Delta\theta}\mathbf{f})_l$$

To accurately capture these effects, use upstream finite differences for each of f_x and f_y:

$$\varphi'(s) = \frac{\varphi(s) - \varphi(s - \Delta s)}{\Delta s} + O(\Delta s),$$
$$\varphi'(s) = \frac{1.5\varphi(s) - 2\varphi(s - \Delta s) + 0.5\varphi(s - 2\Delta s)}{\Delta s} + O(\Delta s^2).$$

Choose sign of Δs based on signs of $(\cos(\theta_l), \sin(\theta_l))$.

An angular relaxation scheme

Consider block ordering of equations by Γ_{n_θ}:

$$\begin{bmatrix} D_{-\frac{n_\theta}{2}+1} + Q_0 & Q_1 & \cdots & Q_{-1} \\ Q_{-1} & D_{-\frac{n_\theta}{2}+2} + Q_0 & \cdots & Q_{-2} \\ & \ddots & \ddots & \vdots \\ Q_1 & \cdots & Q_{-1} & D_{\frac{n_\theta}{2}} + Q_0 \end{bmatrix} \begin{bmatrix} f_{-\frac{n_\theta}{2}+1} \\ f_{-\frac{n_\theta}{2}+2} \\ \vdots \\ f_{\frac{n_\theta}{2}} \end{bmatrix}$$

For each l, can order f_l so that $D_l + Q_0$ is lower triangular

- Block Jacobi solves can be done exactly
- Choose Red-Black (or Black-Red) ordering for efficiency of the resulting multigrid algorithm

Performance of relaxation

Test Problem with smooth broad beam, not grid-aligned:

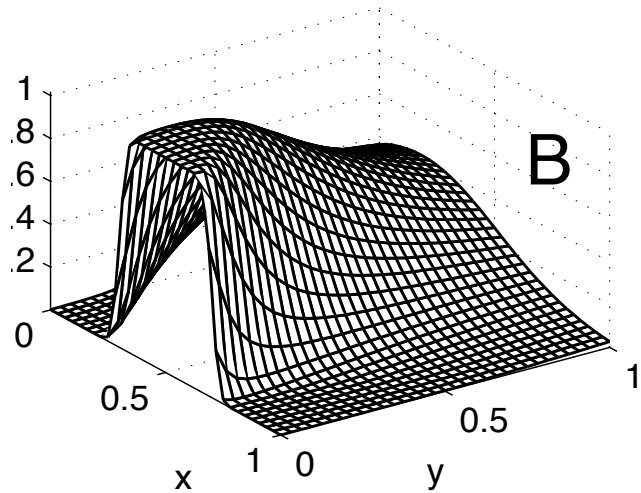

Screened Rutherford scattering

	$n_\theta = 32$	$n_\theta = 64$	$n_\theta = 128$	$n_\theta = 256$	$n_\theta = 512$
$n_s = 32$	0.304	0.662	0.953	0.977	0.988
$n_s = 64$	0.299	0.652	0.943	0.971	0.984
$n_s = 128$	0.294	0.642	0.930	0.963	0.977
$n_s = 256$	0.290	0.633	0.917	0.951	0.969
$n_s = 512$	0.286	0.624	0.903	0.938	0.958

Coarsening in angle

Performance of relaxation seems independent of n_s

Idea: Coarsen only in θ.

- Relaxation damps all errors in x and y
- Elliptic character means Jacobi smooths in θ

Angular coupling has a constant stencil, so try to use simple grid-transfers

- Linear interpolation
- Full-weighting restriction
- Rediscretization for coarse-grid operators

J. Morel and T. Manteuffel, Nuc. Sci. and Eng., 1991, **107**:330-342

S. Vandewalle and G. Horton, Computing, 1995, **54**:317-330

Complication: boundary conditions

Boundary values are prescribed only at inflow boundaries

Natural choice: if $(\cos(\theta_l), \sin(\theta_l))$ points into domain at $(x, y) \in \partial\Omega$, prescribe $f(x, y, \theta_l)$

Difficulty: What to do at $\theta = -\frac{\pi}{2}, 0, \frac{\pi}{2}, \pi$?

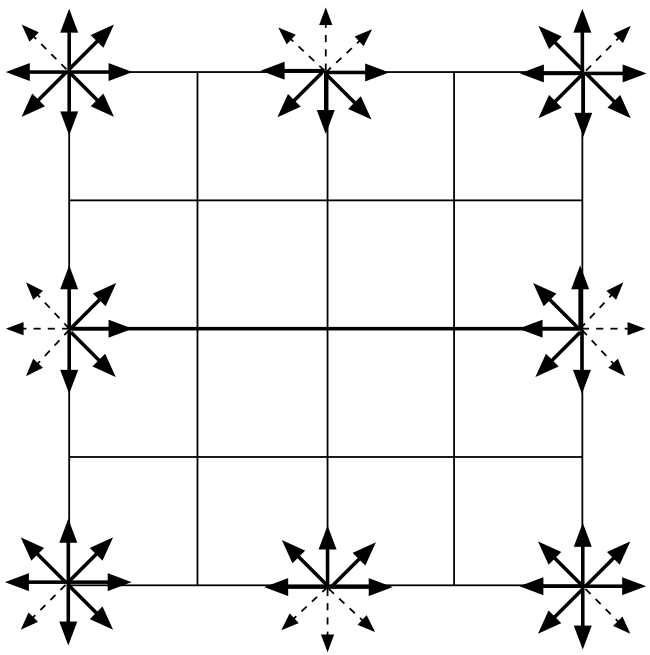

Complication: boundary conditions

Boundary values are prescribed only at inflow boundaries

Natural choice: if $(\cos(\theta_l), \sin(\theta_l))$ points into domain at $(x, y) \in \partial\Omega$, prescribe $f(x, y, \theta_l)$
Difficulty: What to do at $\theta = -\frac{\pi}{2}, 0, \frac{\pi}{2}, \pi$?

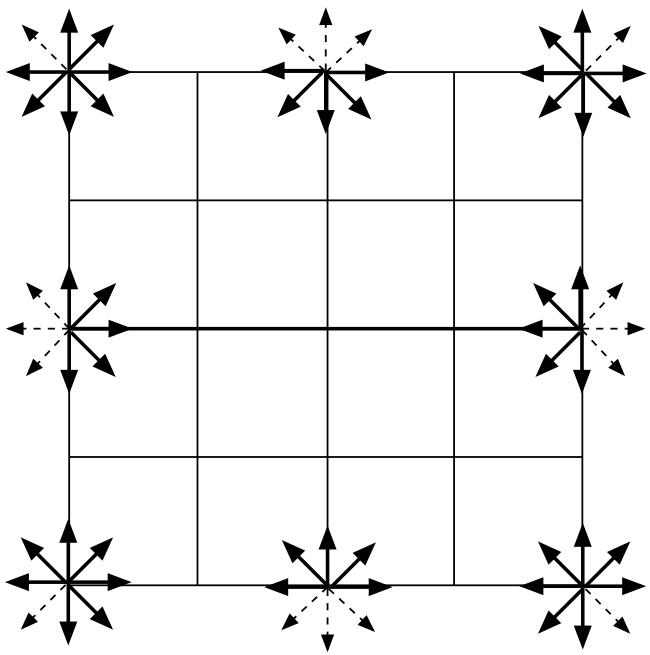

Possible Solutions:

1. Carefully define transfer operators for θ_l near transitions from inflow to outflow
2. Redefine "inflow" and "outflow" so that simple transfer operators don't mix them

Numerical results

Test Problem with smooth broad beam, not grid-aligned:

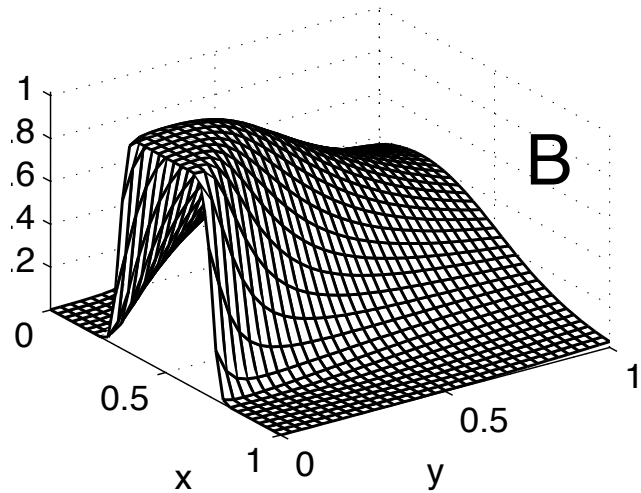

Effective convergence factors for V(0,1) cycles
Screened Rutherford scattering

	$n_\theta = 32$	$n_\theta = 64$	$n_\theta = 128$	$n_\theta = 256$	$n_\theta = 512$
$n_s = 32$	0.698	0.702	0.701	0.706	0.714
$n_s = 64$	0.701	0.707	0.705	0.706	0.712
$n_s = 128$	0.703	0.708	0.714	0.706	0.710
$n_s = 256$	0.706	0.708	0.715	0.708	0.711
$n_s = 512$	0.708	0.709	0.726	0.712	0.711

Numerical results

Dependence on mean free path for $n_s = n_\theta = 128$:

$\overline{\lambda}$	10^{-1}	10^{-2}	10^{-3}	10^{-4}	10^{-5}	10^{-6}	10^{-7}
$\left(\overline{\rho}_{1,24}\right)^{1/4}$	0.704	0.704	0.706	0.713	0.716	0.717	0.717

Performance for 3-point Fokker-Planck Discretization:

	$n_\theta = 32$	$n_\theta = 64$	$n_\theta = 128$	$n_\theta = 256$	$n_\theta = 512$
$n_s = 32$	0.699	0.699	0.702	0.709	0.718
$n_s = 64$	0.702	0.702	0.703	0.708	0.716
$n_s = 128$	0.704	0.704	0.705	0.708	0.714
$n_s = 256$	0.705	0.707	0.707	0.708	0.713
$n_s = 512$	0.708	0.709	0.724	0.709	0.713

C. Börgers and S. MacLachlan, J. Comp. Phys 2010, **229**:2914-2931

Numerical results

Performance for Henyey-Greenstein scattering

	$n_\theta = 32$	$n_\theta = 64$	$n_\theta = 128$	$n_\theta = 256$	$n_\theta = 512$
$n_s = 32$	0.489	0.497	0.547	0.570	0.588
$n_s = 64$	0.493	0.496	0.543	0.567	0.586
$n_s = 128$	0.496	0.497	0.539	0.563	0.582
$n_s = 256$	0.500	0.500	0.535	0.559	0.578
$n_s = 512$	0.503	0.505	0.531	0.555	0.574

C. Börgers and S. MacLachlan, J. Comp. Phys 2010, **229**:2914-2931

Numerical results

Performance for screened Rutherford with 1% Catastrophic collisions

	$n_\theta = 32$	$n_\theta = 64$	$n_\theta = 128$	$n_\theta = 256$	$n_\theta = 512$
$n_s = 32$	0.687	0.725	0.693	0.697	0.719
$n_s = 64$	0.688	0.760	0.750	0.699	0.713
$n_s = 128$	0.691	0.789	0.812	0.767	0.722
$n_s = 256$	0.693	0.810	0.870	0.841	0.797
$n_s = 512$	0.696	0.824	0.919	0.911	

Obvious question

Why?

Obvious question

Why?

What is causing these variations in performance?

- Determined by scattering kernels, but how do these change linear system?
- Can relaxation/coarse-grid correction be adapted to improve performance?
- How will performance change as we go to transport in three spatial dimensions?

Look to local Fourier analysis to gain insight

$$\cos(\theta) f_x + \sin(\theta) f_y = Qf$$

Further simplification

Fixing $\theta_0 \in (-\pi, \pi]$ as direction of transport in convective term gives problem with one angular and one spatial variable
Taking $\theta_0 = 0$ gives

$$f_x = Qf, \quad \text{or,} \quad f_x = k\frac{\partial^2 f}{\partial \theta^2}.$$

Further simplification

Fixing $\theta_0 \in (-\pi, \pi]$ as direction of transport in convective term gives problem with one angular and one spatial variable
Taking $\theta_0 = 0$ gives

$$f_x = Qf, \quad \text{or,} \quad f_x = k\frac{\partial^2 f}{\partial \theta^2}.$$

Change variables: x becomes t and θ becomes x

Further simplification

Fixing $\theta_0 \in (-\pi, \pi]$ as direction of transport in convective term gives problem with one angular and one spatial variable
Taking $\theta_0 = 0$ gives

$$f_x = Qf, \quad \text{or,} \quad f_x = k\frac{\partial^2 f}{\partial \theta^2}.$$

Change variables: x becomes t and θ becomes x

- model problem I:

$$u_t = Qu \tag{1}$$

- model problem II: heat equation

$$u_t = ku_{xx}, \quad k > 0 \tag{2}$$

IC in t, periodic BC in x

Discrete model problems: BDF1 in time

Discretize on rectangular $n_x \times n_t$ space-time grid, giving

$$\underbrace{\left(I_{n_x} \otimes D - Q \otimes I_{n_t}\right)}_{=:A} u = b$$

$$D = \frac{1}{\Delta t}\begin{bmatrix} 1 & & & & \\ -1 & 1 & & & \\ & -1 & 1 & & \\ & & -1 & 1 & \\ & & & \ddots & \ddots \end{bmatrix} \quad Q = \begin{bmatrix} q_0 & q_1 & q_2 & \cdots & q_{-1} \\ q_{-1} & q_0 & q_1 & \cdots & q_{-2} \\ q_{-2} & q_{-1} & q_0 & \cdots & q_{-3} \\ \vdots & & \ddots & \ddots & \vdots \\ q_1 & q_2 & \cdots & q_{-1} & q_0 \end{bmatrix}$$

$$q_m = \frac{1}{n_x} \sum_{n=-n_x/2+1}^{n_x/2} \frac{\widehat{p}_n - 1}{\overline{\lambda}} \cos(nm\Delta x); \; \widehat{p}_n = \int_{-\pi}^{\pi} e^{-in\eta} p(\eta) \, d\eta$$

Discrete model problems: BDF2 in time

Discretize on rectangular $n_x \times n_t$ space-time grid, giving

$$\underbrace{\left(I_{n_x} \otimes D - Q \otimes I_{n_t}\right)}_{=:A} u = b$$

$$D = \frac{1}{\Delta t}\begin{bmatrix} 1.5 & & & & \\ -2 & 1.5 & & & \\ 0.5 & -2 & 1.5 & & \\ & 0.5 & -2 & 1.5 & \\ & & & \ddots & \ddots \end{bmatrix} \quad Q = \begin{bmatrix} q_0 & q_1 & q_2 & \cdots & q_{-1} \\ q_{-1} & q_0 & q_1 & \cdots & q_{-2} \\ q_{-2} & q_{-1} & q_0 & \cdots & q_{-3} \\ \vdots & & \ddots & \ddots & \vdots \\ q_1 & q_2 & \cdots & q_{-1} & q_0 \end{bmatrix}$$

$$q_m = \frac{1}{n_x} \sum_{n=-n_x/2+1}^{n_x/2} \frac{\widehat{p}_n - 1}{\overline{\lambda}} \cos(nm\Delta x); \; \widehat{p}_n = \int_{-\pi}^{\pi} e^{-in\eta} p(\eta) \, d\eta$$

Relaxation schemes

Relaxation schemes are red-black zebra line-relaxations with lines parallel to the time-axis (waveform relaxation).

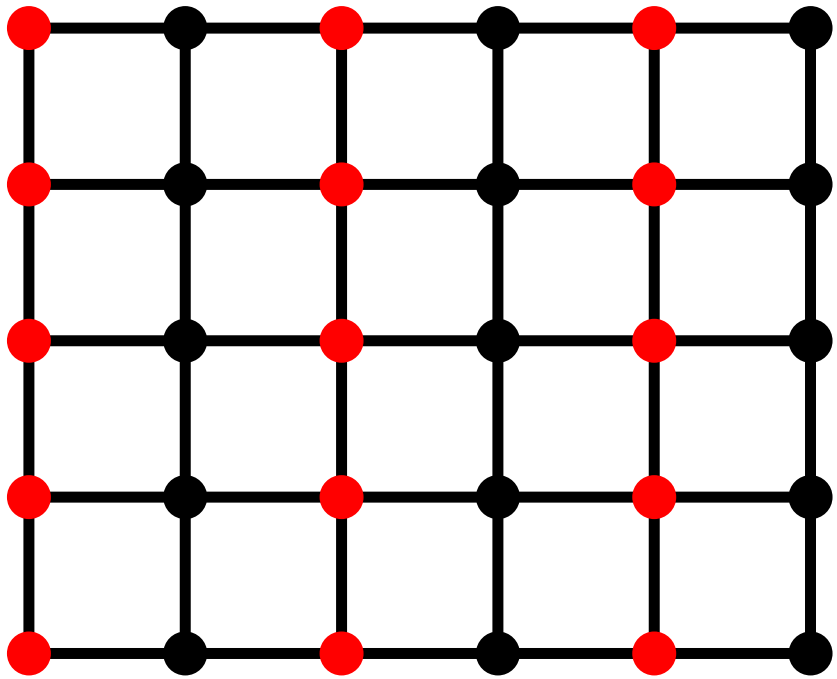

Figure : Red-black ordering for space-time-grid

S. Vandewalle and G. Horton, Computing 1995, **54**:317-330

C. Börgers and S. MacLachlan, J. Comp. Phys 2010, **229**:2914-2931

Relaxation schemes

Red-black smoothing operators are of the form

$$S^{\mathrm{RB}} = S^{\mathrm{BLACK}} S^{\mathrm{RED}},$$

$$S^{\mathrm{RED}} = I - M_R A, \qquad S^{\mathrm{BLACK}} = I - M_B A,$$

$$A = \begin{bmatrix} A_{RR} & A_{RB} \\ A_{BR} & A_{BB} \end{bmatrix}, \quad M_R = \begin{bmatrix} M_{RR}^{-1} & 0 \\ 0 & 0 \end{bmatrix}, \quad M_B = \begin{bmatrix} 0 & 0 \\ 0 & M_{BB}^{-1} \end{bmatrix}.$$

- Jacobi in space-time: $M_{RR} = D_{RR}, \quad M_{BB} = D_{BB}$
- Jacobi in space, Gauss-Seidel in time:
  $M_{RR} = D_{RR} - L_{RR}^{\mathrm{time}}, \quad M_{BB} = D_{BB} - L_{BB}^{\mathrm{time}}$
- Gauss-Seidel in space-time:
  $M_{RR} = D_{RR} - L_{RR}, \quad M_{BB} = D_{BB} - L_{BB}$

Coarse-grid correction

Use a semi-coarsening strategy with coarsening only in the spatial dimension.

Intergrid transfer operators are

- periodic linear interpolation, P
- full-weighting restriction, $R = \frac{1}{2}P^T$

Two-grid iteration matrix

$$\mathbf{M} = \mathbf{S}^{\mathrm{RB}}(\mathbf{I} - \mathbf{P}(\mathbf{A}^{\mathrm{c}})^{-1}\mathbf{R}\mathbf{A})\mathbf{S}^{\mathrm{RB}}$$

Rigorous Fourier analysis

How do relaxation and coarse-grid correction act on errors in an approximation?

- block-circulant matrices with circulant blocks are diagonalized by the Fourier modes

$$\varphi(\boldsymbol{\theta}, x, t) = \mathrm{e}^{-i\frac{\theta_1 x}{\Delta x}}\,\mathrm{e}^{-i\frac{\theta_2 t}{\Delta t}} \quad \text{for } \boldsymbol{\theta} = \left(\frac{2\pi k}{n_x}, \frac{2\pi l}{n_t}\right),\ k, l \in \mathbb{Z},$$

$$k \in \left(-\frac{n_x}{2}, \frac{n_x}{2}\right],\ l \in \left(-\frac{n_t}{2}, \frac{n_t}{2}\right]$$

- expand the error into Fourier modes and determine how relaxation and coarse-grid correction act on these modes
- two-dimensional harmonic spaces are invariant subspaces for RB-relaxations, restriction, and interpolation

---

K. Stüben and U. Trottenberg, Lect. Notes Comp. Sci. Eng. 1982, **960**:1-176

Harmonic modes

Multigrid processing naturally mixes modes

Natural through coarse-grid correction

- Fine-grid modes are aliased when represented on coarse grid
- Connects mode with frequency (θ_x, θ_t) with $(\theta_x \pm \pi, \theta_t)$

Also occurs in red-black relaxation

- Updating alternate points in space

Semicoarsening multigrid is block-diagonalized by Fourier modes, but only 2×2 block size

Fourier analysis for model transport problems: BDF1 in time

We apply red-black-type relaxations to the system

$$\underbrace{\left(I_{n_x} \otimes D \quad - Q \otimes I_{n_t}\right)}_{=:A} u = b.$$

$$A = \begin{bmatrix} \frac{1}{\Delta t} I - Q & & & & \\ -\frac{1}{\Delta t} I & \frac{1}{\Delta t} I - Q & & & \\ & -\frac{1}{\Delta t} I & \frac{1}{\Delta t} I - Q & & \\ & & \ddots & \ddots & \\ & & & -\frac{1}{\Delta t} I & \frac{1}{\Delta t} I - Q \end{bmatrix}$$

Fourier analysis for model transport problems: BDF1 in time

We apply red-black-type relaxations to the system

$$\underbrace{\left(I_{n_x} \otimes D^{\text{per}} - Q \otimes I_{n_t}\right)}_{=:A} u = b.$$

periodicity in time

$$A = \begin{bmatrix} \frac{1}{\Delta t} I - Q & & & & -\frac{1}{\Delta t} I \\ -\frac{1}{\Delta t} I & \frac{1}{\Delta t} I - Q & & & \\ & -\frac{1}{\Delta t} I & \frac{1}{\Delta t} I - Q & & \\ & & \ddots & \ddots & \\ & & & -\frac{1}{\Delta t} I & \frac{1}{\Delta t} I - Q \end{bmatrix}$$

Fourier analysis for model transport problems: BDF2 in time

We apply red-black-type relaxations to the system

$$\underbrace{\left(I_{n_x} \otimes D \quad - Q \otimes I_{n_t}\right)}_{=:A} u = b.$$

$$A = \begin{bmatrix} \frac{3}{2\Delta t} I - Q & & & & \\ -\frac{2}{\Delta t} I & \frac{3}{2\Delta t} I - Q & & & \\ \frac{1}{2\Delta t} I & -\frac{2}{\Delta t} I & \frac{3}{2\Delta t} I - Q & & \\ & \ddots & \ddots & \ddots & \\ & & \frac{1}{2\Delta t} I & -\frac{2}{\Delta t} I & \frac{3}{2\Delta t} I - Q \end{bmatrix}$$

Fourier analysis for model transport problems: BDF2 in time

We apply red-black-type relaxations to the system

$$\underbrace{\left(I_{n_x} \otimes D^{\text{per}} - Q \otimes I_{n_t}\right)}_{=:A} u = b.$$

periodicity in time

$$A = \begin{bmatrix}
\frac{3}{2\Delta t} I - Q & & & \frac{1}{2\Delta t} I & -\frac{2}{\Delta t} I \\
-\frac{2}{\Delta t} I & \frac{3}{2\Delta t} I - Q & & & \frac{1}{2\Delta t} I \\
\frac{1}{2\Delta t} I & -\frac{2}{\Delta t} I & \frac{3}{2\Delta t} I - Q & & \\
& \ddots & \ddots & \ddots & \\
& & \frac{1}{2\Delta t} I & -\frac{2}{\Delta t} I & \frac{3}{2\Delta t} I - Q
\end{bmatrix}$$

Local Fourier analysis (LFA)

As opposed to rigorous Fourier analysis, LFA can be applied to noncirculant operators.

- assume that relaxation and coarse-grid correction are local processes
- consider infinite grid

$$\Omega_h = \left\{(x,t) = (k\Delta x, l\Delta t),\ (k,l) \in \mathbb{Z}^2\right\}$$

- neglect boundaries and boundary conditions
- any infinite-grid block Toeplitz operator with Toeplitz blocks is diagonalized by grid functions

$$\varphi(\boldsymbol{\theta}, x, t) = \mathrm{e}^{-i\frac{\theta_1 x}{\Delta x}}\,\mathrm{e}^{-i\frac{\theta_2 t}{\Delta t}} \quad \text{for } \boldsymbol{\theta} \in (-\pi,\pi]^2,\ (x,t) \in \Omega_h$$

A. Brandt, Math. Comp. **31** (1977), no. 138, pp. 333-390

Local Fourier analysis: a predictive tool

Any grid function is represented as a linear combination of the Fourier modes on the infinite grid

- extend the matrix, A, relaxation and coarse-grid correction operators to the infinite grid Ω_h
- two-dimensional harmonic spaces are invariant subspaces for RB-relaxation and coarse-grid correction
- use continuous Fourier modes to block-diagonalize infinite-grid operators
- sample continuous frequency on a finite grid

The spectral radius of the transformed operators gives insight into the asymptotic convergence behavior.

LFA for model transport problems

Periodic space-time grid

- for any scattering kernel, Q, is circulant
- periodic-in-time matrix, D, is circulant

LFA is exact for Jacobi and should be good for Gauss-Seidel.

LFA for model transport problems

Periodic space-time grid

- for any scattering kernel, Q, is circulant
- periodic-in-time matrix, D, is circulant

LFA is exact for Jacobi and should be good for Gauss-Seidel.

Periodicity in space only

- Q is circulant
- D is a Jordan block $\rightsquigarrow$ not diagonalizable

LFA should good only for large grids.
Q1: What does "large" mean?
Q2: Is convergence good enough to understand results of transport problems?

LFA for the heat equation

- standard central differences for spatial operator
- BDF1, BDF2 for the time-discretization
- semi-coarsening (coarsening only in the spatial dimension)
- smoother in the multigrid waveform relaxation method is a zebra Gauss-Seidel method

Our approach:

- First fix Δx, Δt, look at results for varying n_t
- compare with results from Vandewalle & Horton for $n_x = n_t = 128$, varying Δt
- Look at variation w.r.t. $T = n_t \times \Delta t$

S. Vandewalle and G. Horton, Computing 1995, **54**:317-330

Heat equation: red-black Jacobi

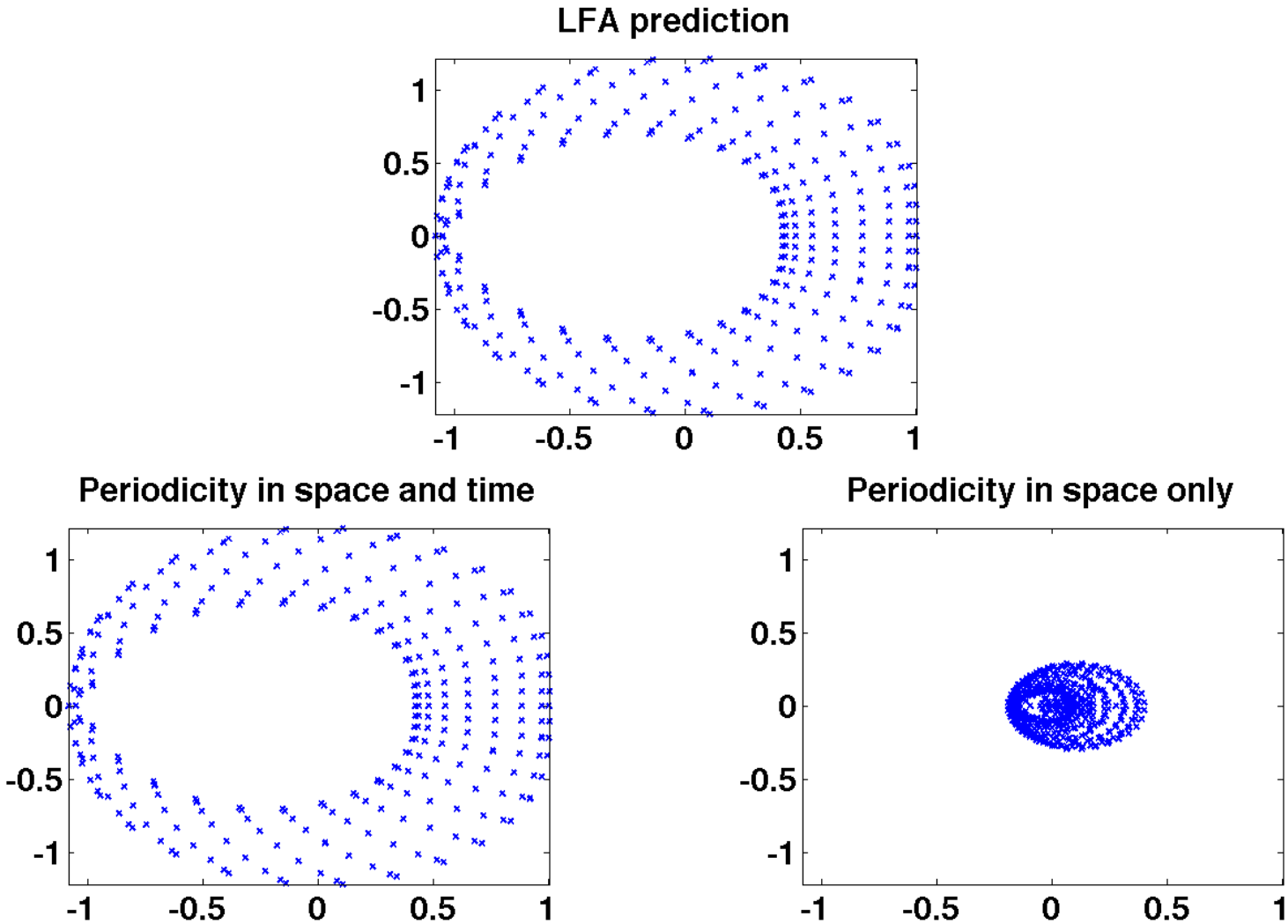

Figure : Numerical results for $n_x = 16,\ n_t = 32$

Heat equation: red-black Jacobi

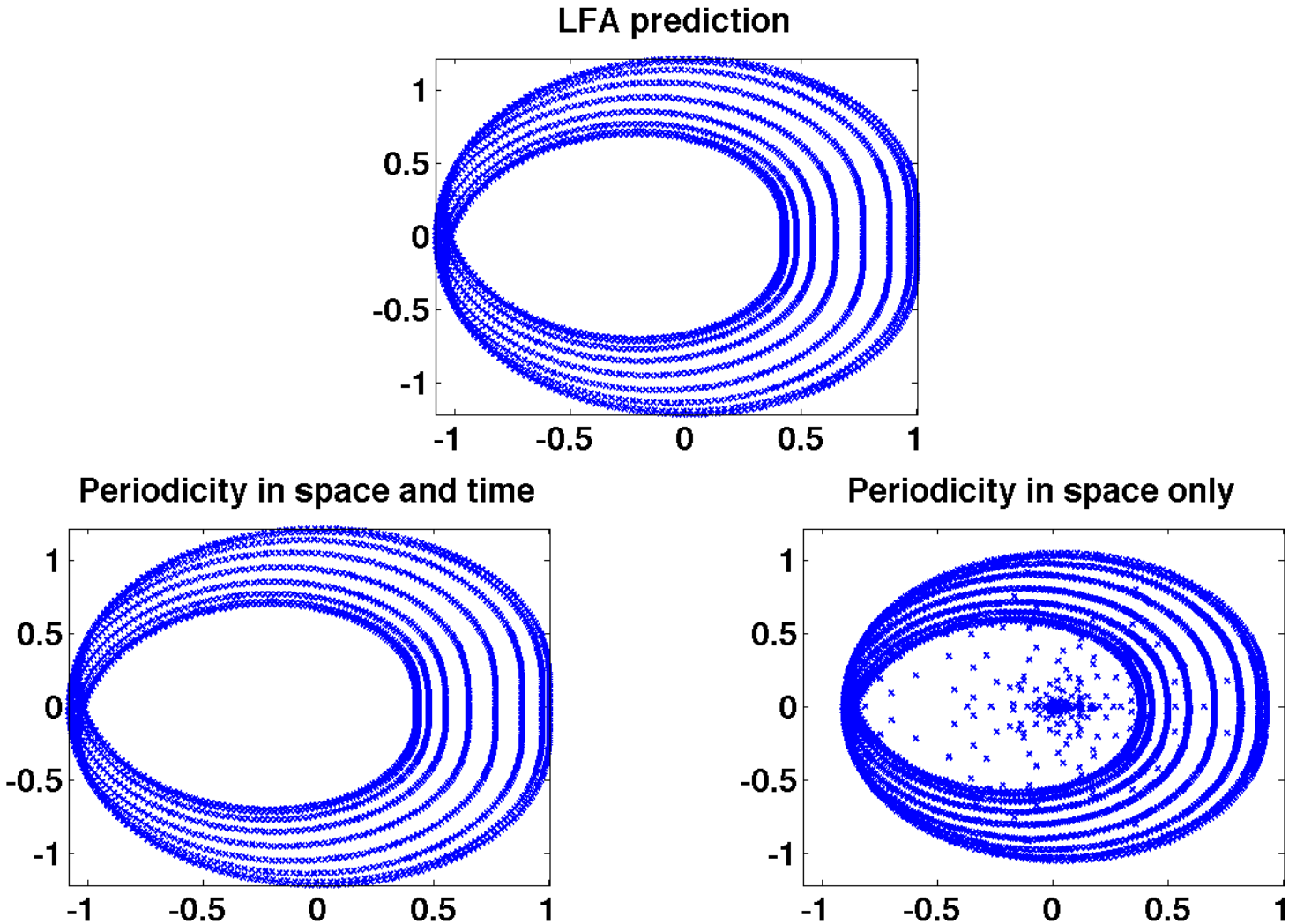

Figure : Numerical results for $n_x = 16,\ n_t = 256$

Heat equation: red-black Jacobi

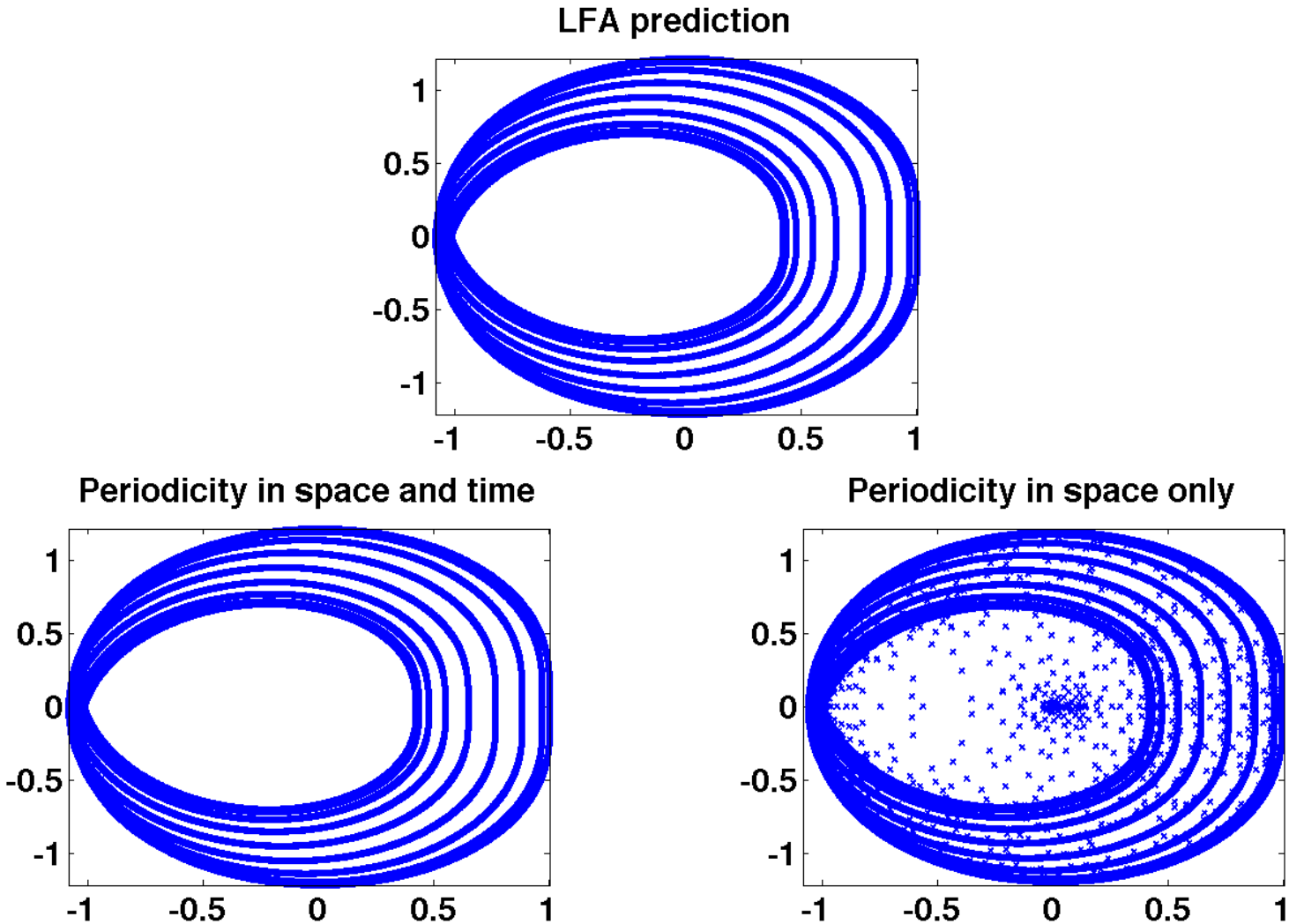

Figure : Numerical results for $n_x = 16,\ n_t = 2048$

Heat equation: red-black line Gauss-Seidel

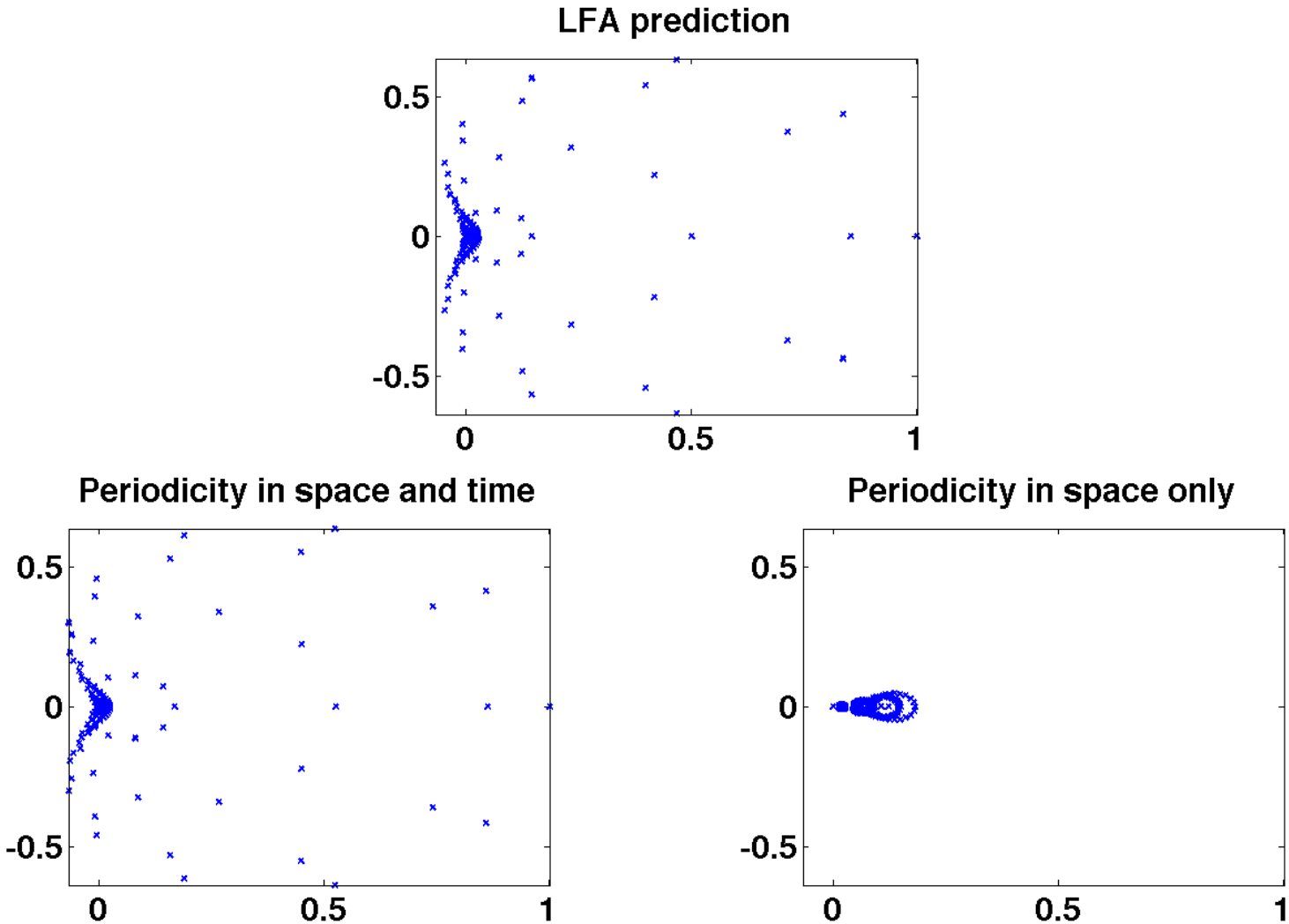

Figure : Numerical results for $n_x = 16,\ n_t = 32$

Heat equation: red-black line Gauss-Seidel

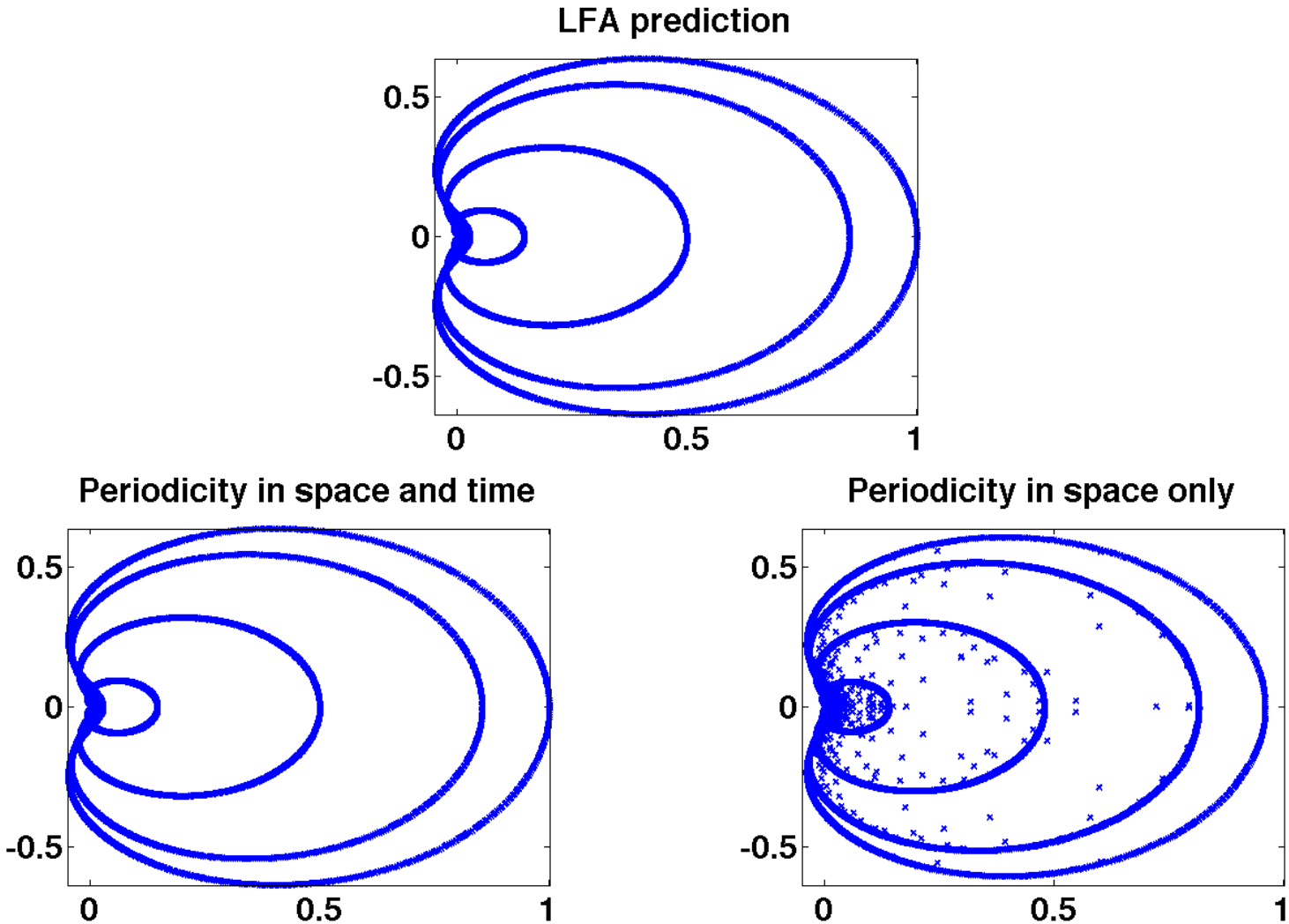

Figure : Numerical results for $n_x = 16,\ n_t = 2048$

Heat equation: two-grid

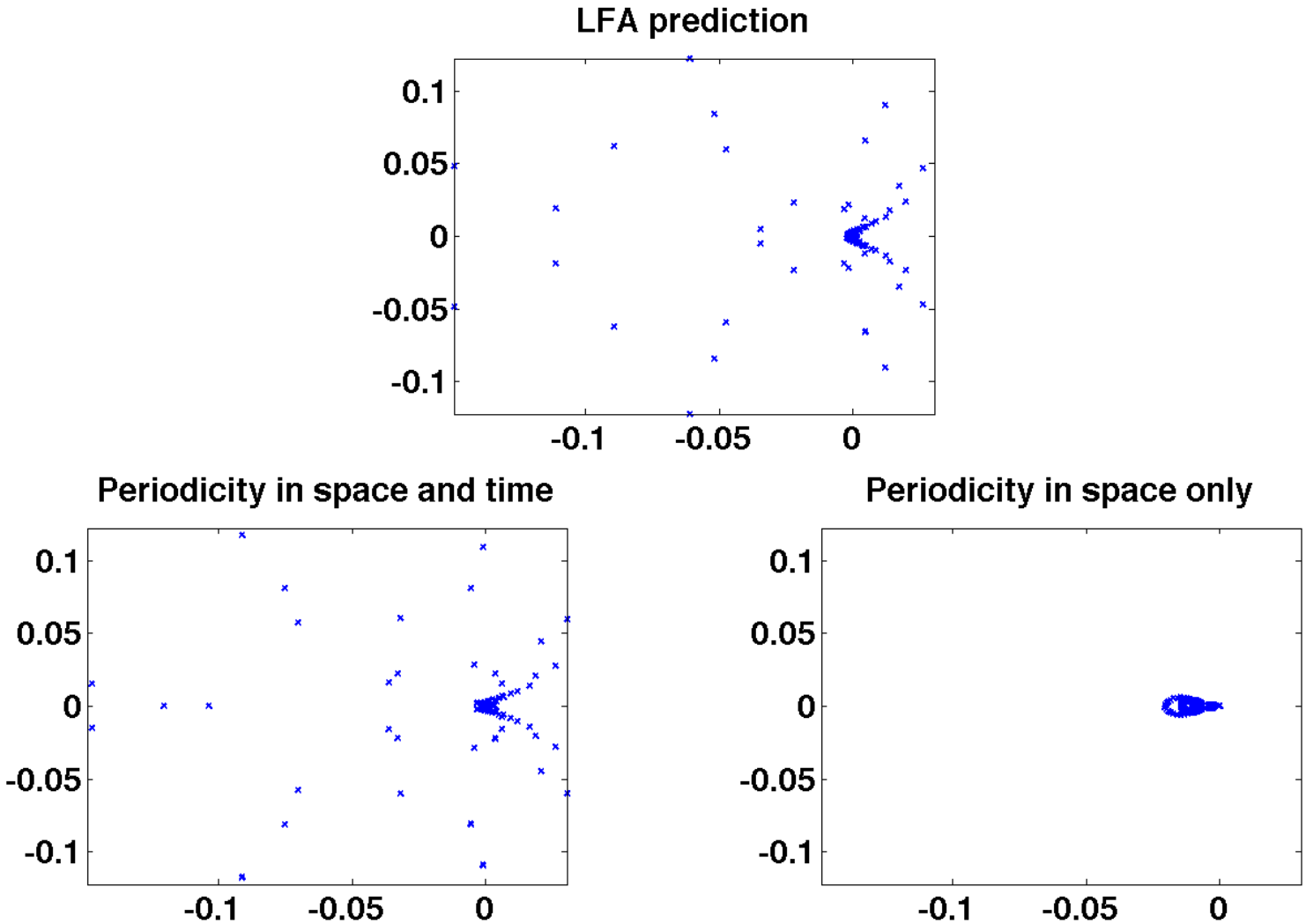

Figure : Numerical results for $n_x = 16,\ n_t = 32$

Heat equation: two-grid

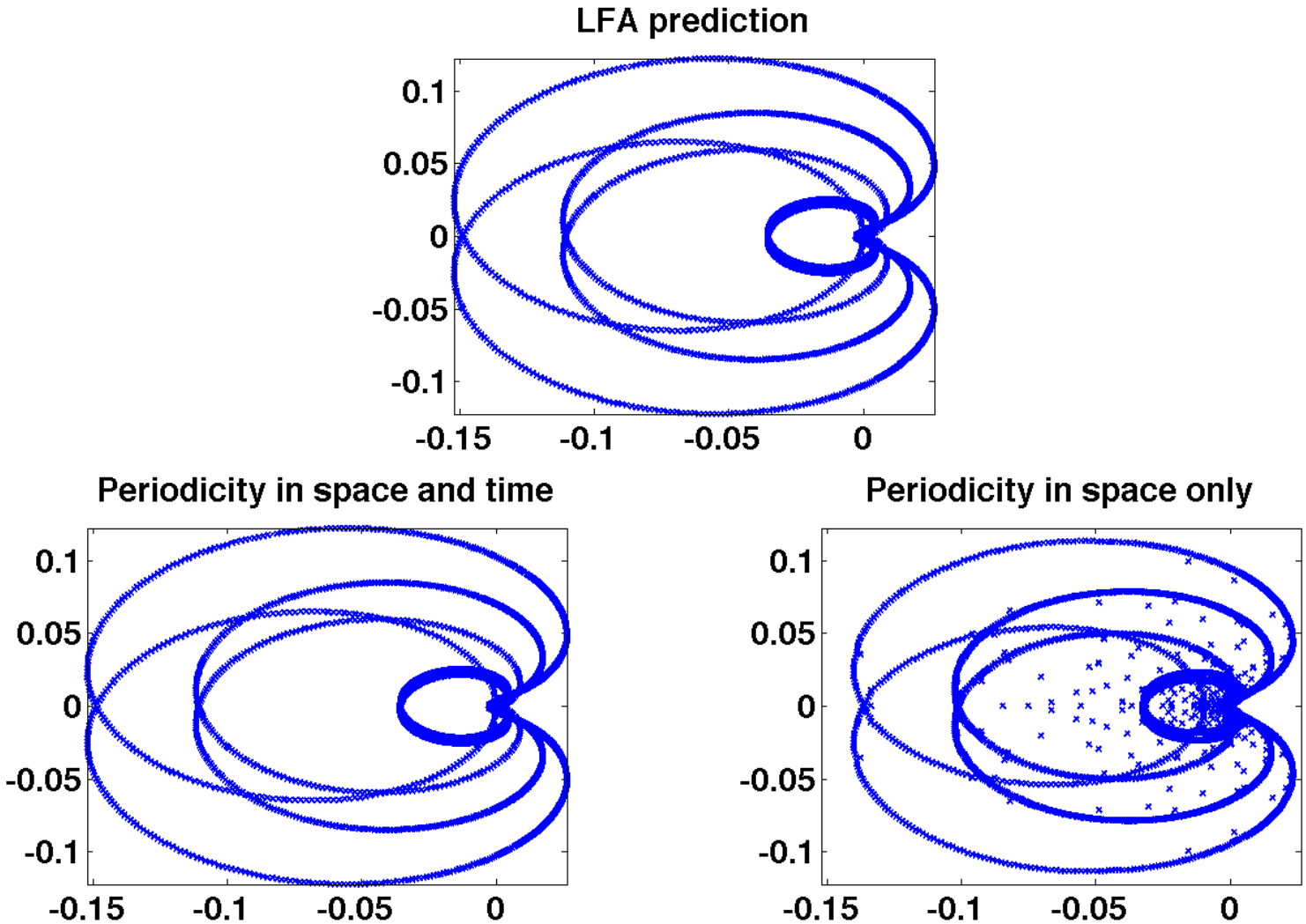

Figure : Numerical results for $n_x = 16,\ n_t = 2048$

Comparison: BDF1 in time

- fix mesh size $n_x = n_t = 128$, fix Δx, vary Δt
- define mesh aspect ratio $\lambda_h := \Delta t/(\Delta x)^2$
- measured residual convergence factors from Vandewalle & Horton
- LFA prediction with "enough" points in time-Fourier direction
- analytical computation of spectral radius

$\log_2(\lambda_h)$	-6	-3	0	3	6	9
average convergence factor	.02	.11	.08	.04	.01	.00
LFA prediction	.06	.14	.09	.04	.01	.00
analytical computation	.00	.02	.07	.04	.01	.00

Table : Results for two-grid with Gauss-Seidel in space-time

S. Vandewalle and G. Horton, Computing 1995, **54**:317-330

Comparison: BDF2 in time

- fix mesh size $n_x = n_t = 128$, fix Δx, vary Δt
- define mesh aspect ratio $\lambda_h := \Delta t/(\Delta x)^2$
- measured residual convergence factors from Vandewalle & Horton
- LFA prediction with "enough" points in time-Fourier direction
- analytical computation of spectral radius

$\log_2(\lambda_h)$	-6	-3	0	3	6	9
average convergence factor	.02	.12	.12	.05	.01	.00
LFA prediction	.07	.16	.14	.06	.01	.00
analytical computation	.00	.01	.08	.05	.01	.00

Table : Results for two-grid with Gauss-Seidel in space-time

S. Vandewalle and G. Horton, Computing 1995, **54**:317-330

Screened Rutherford: two-grid

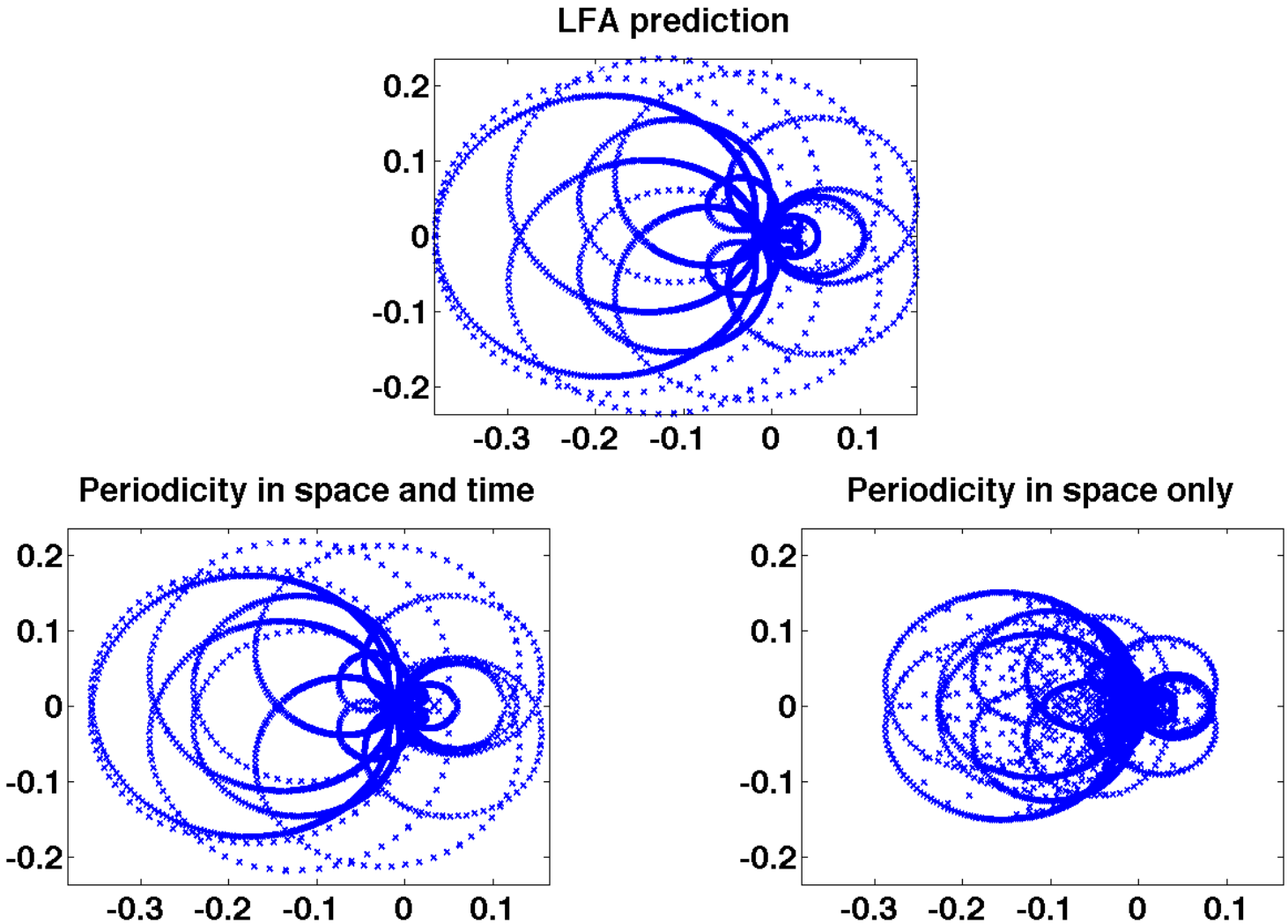

Figure : Numerical results for $n_x = 16,\ n_t = 2048$

Henyey-Greenstein: two-grid

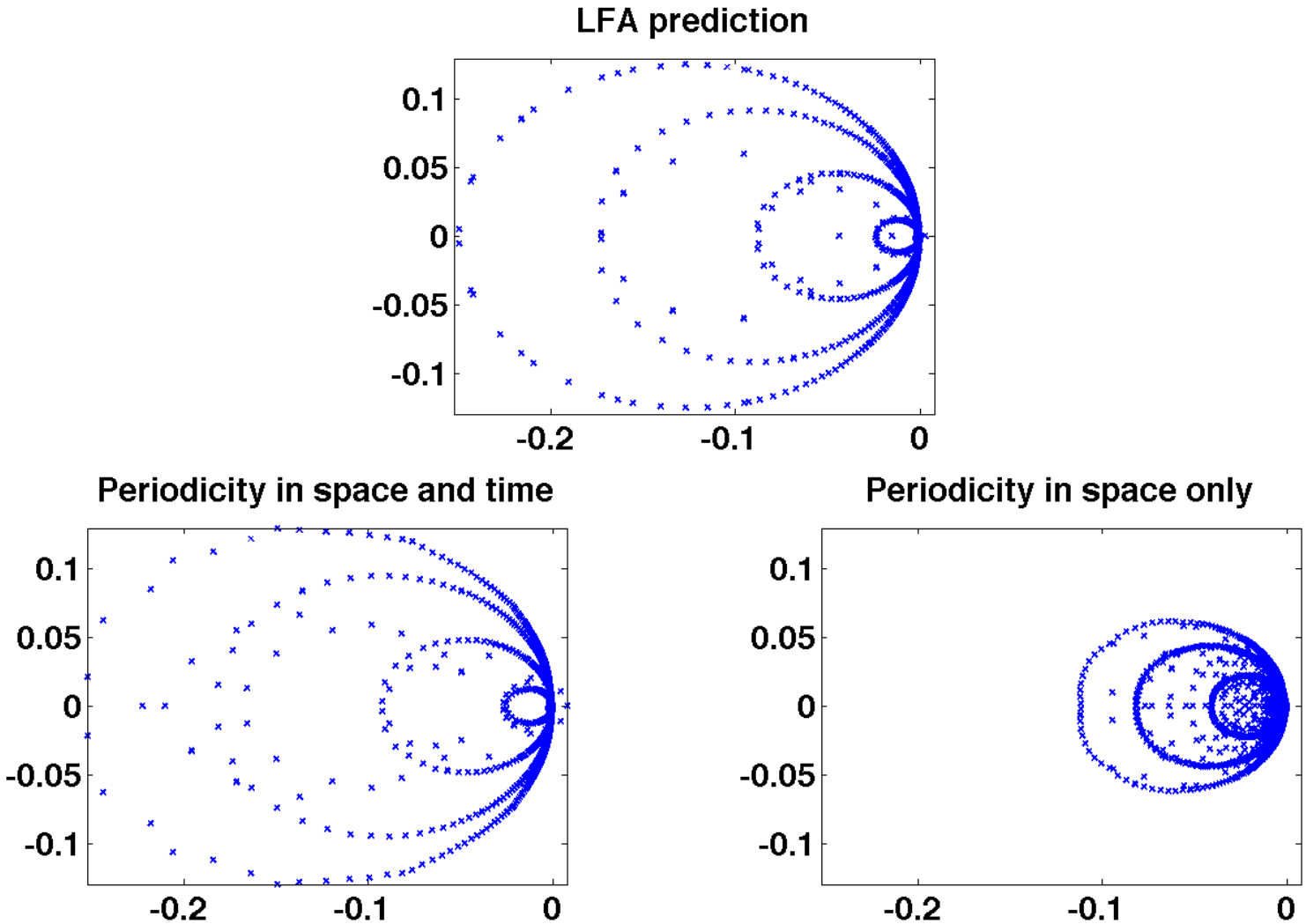

Figure : Numerical results for $n_x = 16,\ n_t = 2048$

Henyey-Greenstein, varying n_t

Fix Δt, vary integration time, $T = n_t \times \Delta_t$

Δt	$n_x = 32$	$n_x = 64$	$n_x = 128$	$n_x = 256$	$n_x = 512$
$1/128$	0.045	0.089	0.161	0.238	0.237
$1/256$	0.046	0.089	0.162	0.238	0.237
$1/512$	0.046	0.089	0.162	0.238	0.237

$$T = 1$$

Evaluating LFA functional at $n_x \times (T \times n_t)$ Fourier points

Henyey-Greenstein, varying n_t

Fix Δt, vary integration time, $T = n_t \times \Delta_t$

Δt	$n_x = 32$	$n_x = 64$	$n_x = 128$	$n_x = 256$	$n_x = 512$
$1/128$	0.089	0.162	0.238	0.238	0.249
$1/256$	0.089	0.162	0.238	0.238	0.249
$1/512$	0.089	0.162	0.238	0.238	0.249

$$T = 2$$

Evaluating LFA functional at $n_x \times (T \times n_t)$ Fourier points

Henyey-Greenstein, varying n_t

Fix Δt, vary integration time, $T = n_t \times \Delta_t$

Δt	$n_x = 32$	$n_x = 64$	$n_x = 128$	$n_x = 256$	$n_x = 512$
$1/128$	0.162	0.238	0.238	0.250	0.249
$1/256$	0.162	0.238	0.238	0.250	0.249
$1/512$	0.162	0.238	0.238	0.250	0.249

$$T = 4$$

Evaluating LFA functional at $n_x \times (T \times n_t)$ Fourier points

Henyey-Greenstein, varying n_t

Fix Δt, vary integration time, $T = n_t \times \Delta_t$

Δt	$n_x = 32$	$n_x = 64$	$n_x = 128$	$n_x = 256$	$n_x = 512$
$1/128$	0.239	0.238	0.250	0.250	0.249
$1/256$	0.239	0.238	0.250	0.250	0.249
$1/512$	0.239	0.238	0.250	0.250	0.249

$$T = 8$$

Evaluating LFA functional at $n_x \times (T \times n_t)$ Fourier points

Henyey-Greenstein, varying n_t

Fix Δt, vary integration time, $T = n_t \times \Delta_t$

Δt	$n_x = 32$	$n_x = 64$	$n_x = 128$	$n_x = 256$	$n_x = 512$
$1/128$	0.239	0.250	0.250	0.250	0.249
$1/256$	0.239	0.250	0.250	0.250	0.249
$1/512$	0.239	0.250	0.250	0.250	0.249

$$T = 16$$

Evaluating LFA functional at $n_x \times (T \times n_t)$ Fourier points

Comparison with numerical rates

Compare these with flatland transport model
LFA predictions:

- diffusion/Fokker-Planck: $\rho_{LFA} = 0.25$
- Screened Rutherford: $\rho_{LFA} = 0.36$
- Henyey-Greenstein: $\rho_{LFA} = 0.25$

Numerical rates:

- Fokker-Planck: $\rho_{comp} = 0.25$
- Screened Rutherford: $\rho_{comp} = 0.25$
- Henyey-Greenstein: $\rho_{comp} = 0.11$

C. Börgers and S. MacLachlan, J. Comp. Phys 2010, **229**:2914-2931

Comparison with numerical rates

Compare these with flatland transport model
LFA predictions:

- diffusion/Fokker-Planck: $\rho_{LFA} = 0.25$
- Screened Rutherford: $\rho_{LFA} = 0.36$
- Henyey-Greenstein: $\rho_{LFA} = 0.25$

Numerical rates:

- Fokker-Planck: $\rho_{comp} = 0.25$
- Screened Rutherford: $\rho_{comp} = 0.25$
- Henyey-Greenstein: $\rho_{comp} = 0.11$

Still missing something...

C. Börgers and S. MacLachlan, J. Comp. Phys 2010, **229**:2914-2931

One possibility...

All of our LFA is based on assuming fixed $\theta_0 = 0$ in

$$\cos(\theta_0) f_x + \sin(\theta_0) f_y = Qf$$

Standard approach for LFA of variable-coefficient equations is to apply LFA to each distinct stencil, then take worst case

One possibility...

All of our LFA is based on assuming fixed $\theta_0 = 0$ in

$$\cos(\theta_0) f_x + \sin(\theta_0) f_y = Qf$$

Standard approach for LFA of variable-coefficient equations is to apply LFA to each distinct stencil, then take worst case

However, LFA isn't working so well anyway, so let's start again

Combining analysis and computation

Look again at matrix structure

Block by angle:

$$\begin{bmatrix} D_{-\frac{n_\theta}{2}+1} + Q_0 & Q_1 & \cdots & Q_{-1} \\ Q_{-1} & D_{-\frac{n_\theta}{2}+2} + Q_0 & \cdots & Q_{-2} \\ & \ddots & \ddots & \vdots \\ Q_1 & \cdots & Q_{-1} & D_{\frac{n_\theta}{2}} + Q_0 \end{bmatrix} \begin{bmatrix} f_{-\frac{n_\theta}{2}+1} \\ f_{-\frac{n_\theta}{2}+2} \\ \vdots \\ f_{\frac{n_\theta}{2}} \end{bmatrix}$$

Combining analysis and computation

Look again at matrix structure

Block by space:

$$\begin{bmatrix} Q+D_{0,0} & 0 & \dots & 0 \\ D_{0,-1} & Q+D_{0,0} & & 0 \\ & \ddots & \ddots & \vdots \\ D_{1-n_s,1-n_s} & \dots & D_{0,-1} & Q+D_{0,0} \end{bmatrix} \begin{bmatrix} f_{1,1} \\ f_{1,2} \\ \vdots \\ f_{n_s,n_s} \end{bmatrix}$$

Multi-block Toeplitz, with Block-Toeplitz with circulant blocks multi-block structure

Combining analysis and computation

Look again at matrix structure

Easier to see for heat equation

$$A\mathbf{f} = \begin{bmatrix} Q + D_0 & 0 & \dots & 0 \\ D_{-1} & Q + D_0 & & 0 \\ & \ddots & \ddots & \vdots \\ D_{1-n_t} & \dots & D_{-1} & Q + D_0 \end{bmatrix} \begin{bmatrix} f_1 \\ f_2 \\ \vdots \\ f_{n_t} \end{bmatrix}$$

Block Toeplitz with circulant blocks

Combining analysis and computation

Look again at matrix structure

Easier to see for heat equation

$$A\mathbf{f} = \begin{bmatrix} Q + D_0 & 0 & \dots & 0 \\ D_{-1} & Q + D_0 & & 0 \\ & \ddots & \ddots & \vdots \\ D_{1-n_t} & \dots & D_{-1} & Q + D_0 \end{bmatrix} \begin{bmatrix} f_1 \\ f_2 \\ \\ \vdots \\ \\ f_{n_t} \end{bmatrix}$$

Block Toeplitz with circulant blocks

Diagonalize circulant blocks with Fourier, then look again

Finding block structure

Look to block diagonalize A

$$A = \begin{bmatrix} Q + D_0 & 0 & \cdots & 0 \\ D_{-1} & Q + D_0 & & 0 \\ & \ddots & \ddots & \vdots \\ D_{1-n_t} & \cdots & D_{-1} & Q + D_0 \end{bmatrix}$$

Finding block structure

Look to block diagonalize A

$$F^{-1}AF = \begin{bmatrix} \Lambda + D_0 & 0 & \dots & 0 \\ D_{-1} & \Lambda + D_0 & & 0 \\ & \ddots & \ddots & \vdots \\ D_{1-n_t} & \dots & D_{-1} & \Lambda + D_0 \end{bmatrix}$$

Block Toeplitz matrix with diagonal blocks

Finding block structure

Look to block diagonalize A

$$P^{-1}F^{-1}AFP = \begin{bmatrix} B_1 & 0 & \dots & 0 \\ 0 & B_2 & & 0 \\ & \ddots & \ddots & \vdots \\ 0 & \dots & 0 & B_{n_x} \end{bmatrix}$$

for $B_i = \begin{bmatrix} \lambda_i + d_0 & 0 & \dots & 0 \\ d_{-1} & \lambda_i + d_0 & & 0 \\ & \ddots & \ddots & \vdots \\ d_{1-n_t} & \dots & d_{-1} & \lambda_i + d_0 \end{bmatrix}$

Block diagonal matrix with Toeplitz blocks

Semi-algebraic mode analysis (SAMA)

Recognize that computing eigenvalues of

$$B_i = \begin{bmatrix} \lambda_i + d_0 & 0 & \dots & 0 \\ d_{-1} & \lambda_i + d_0 & & 0 \\ & \ddots & \ddots & \vdots \\ d_{1-n_t} & \dots & d_{-1} & \lambda_i + d_0 \end{bmatrix}$$

is not difficult

Semi-algebraic approach to mode analysis:

- Use Fourier bases to resolve circulant behaviour
- Use numerical computation to resolve non-circulant terms

Provides both exact eigenvalue expressions and insight into local mode analysis

Semi-algebraic mode analysis (SAMA)

Recognize that computing eigenvalues of

$$B_i = \begin{bmatrix} \lambda_i + d_0 & 0 & \dots & 0 \\ d_{-1} & \lambda_i + d_0 & & 0 \\ & \ddots & \ddots & \vdots \\ d_{1-n_t} & \dots & d_{-1} & \lambda_i + d_0 \end{bmatrix}$$

is not difficult (they are all $\lambda_i + d_0$)

Semi-algebraic approach to mode analysis:

- Use Fourier bases to resolve circulant behaviour
- Use numerical computation to resolve non-circulant terms

Provides both exact eigenvalue expressions and insight into local mode analysis

Summary

- "Flatland" PDE model of Boltzmann Transport
- Collision operator is elliptic, model is mixed elliptic-hyperbolic
- Angular multigrid based on downstream relaxation
- Efficient and scalable solution algorithm
- Problem for which classical LFA unhelpful
- New mode analysis approaches look promising

Summary

- "Flatland" PDE model of Boltzmann Transport
- Collision operator is elliptic, model is mixed elliptic-hyperbolic
- Angular multigrid based on downstream relaxation
- Efficient and scalable solution algorithm
- Problem for which classical LFA unhelpful
- New mode analysis approaches look promising

Future Directions

- Three space dimensions, scattering in S^2
- Local grid refinement in space and angle
- Other discretizations
- Comparison to particle methods